Article:

Nkiaka, E. orcid.org/0000-0001-7362-9430, Bryant, R.G. orcid.org/0000-0001-7943-4781 and Dembélé, M. (2025) Quantifying Sahel runoff sensitivity to climate variability, soil moisture and vegetation changes using analytical methods. Earth Systems and Environment, 9 (1). pp. 491-504. ISSN 2509-9426

https://doi.org/10.1007/s41748-024-00464-3

Earth Systems and Environment
https://doi.org/10.1007/s41748-024-00464-3

ORIGINAL ARTICLE

Quantifying Sahel Runoff Sensitivity to Climate Variability, Soil Moisture and Vegetation Changes Using Analytical Methods

Elias Nkiaka[1,2] · Robert G. Bryant[1] · Moctar Dembélé[3,4]

Received: 20 May 2024 / Revised: 7 August 2024 / Accepted: 1 September 2024

Abstract

Whilst substantial efforts have been deployed to understand the "Sahel hydrological paradox", most of the studies focused on small experimental watersheds around the central and western Sahel. To our knowledge, there is no study on this issue covering all the watersheds located within the Sahelian belt. The absence of relevant studies may be attributed to a sparsity of in situ data leading to a dearth of knowledge on the Sahel hydrology. To fill this knowledge gap, the present study leverages analytical methods and freely available geospatial datasets to understand the effects of climatic factors, soil moisture and vegetation cover changes on surface runoff in 45 watersheds located within the Sahelian belt over two decades (2000–2021). Analyses show increasing trends in annual precipitation and potential evapotranspiration (PET) in more than 80% of the watersheds. Surface runoff, soil moisture (SM), and vegetation cover measured using the normalised difference vegetation index (NDVI) also show increasing trends in all the watersheds. Multivariable linear regression (MLR) analyses reveal that precipitation, PET, SM, and NDVI contribute about 62% of surface runoff variance. Further analyses using MLR, and the partial least squares regression (PLSR) show that precipitation and NDVI are the main factors influencing surface runoff in the Sahel. Elasticity coefficients reveal that a 10% increase in precipitation, SM and NDVI may lead to about 22%, 26% and 45% increase in surface runoff respectively. In contrast, a 10% increase in PET may lead to a 61% decline in surface runoff in the Sahel. This is the first hydrological study covering all the watersheds located within the Sahelian belt with results showing that surface runoff is influenced by climate, SM and NDVI to varying degrees. Given the unique hydrological characteristics of the Sahel, a better understanding of the different factors influencing surface runoff may be crucial for enhancing climate adaptation and ecological restoration efforts in the region such as the Great Green Wall Initiative.

Keywords Analytical methods · Budyko framework · Elasticity concept · Geospatial data · Sahel hydrological paradox · Variable Importance in Projection

1 Introduction

Surface runoff is an important component of the hydrological cycle, crucially important for providing a reliable source of water for domestic consumption; food and hydropower production; and ensuring ecosystems sustainability (Greve et al. 2018; Baggio et al. 2021). According to the Intergovernmental Panel on Climate Change (IPCC) report, climate change is going to alter hydrological conditions in many regions (Mirzabaev et al. 2022). This is especially the case in dryland regions such as the Sahel where climatic factors have substantial impact on surface runoff (Wendling et al. 2019; Gbohoui et al. 2021). Surface runoff is also strongly influenced by soil moisture, landscape characteristics and vegetation cover which all vary in space and time (Liu et al. 2017). Therefore, it is imperative to understand the relative contributions of the different factors on surface runoff as this may be crucial to enhance water management and ecological restoration efforts in dryland areas.

Different methods have been employed to investigate the effects of climate and vegetation cover changes on surface

✉ Elias Nkiaka
e.nkiaka@sheffield.ac.uk

1 Department of Geography, University of Sheffield, Sheffield S10 2TN, UK

2 Department of Geography, Catchments and Coasts Research Group, University of Lincoln, Lincoln, UK

3 International Water Management Institute (IWMI), CSIR Campus, 6 Agostino Neto Road, Accra, Ghana

4 School of Geography and the Environment, University of Oxford, South Parks Road, Oxford, QY OX1, UK

Published online: 16 September 2024

runoff including numerical modelling (Dembélé et al. 2022; Ebodé et al. 2022), experimental approaches involving paired catchment studies and analytical methods (Dey and Mishra 2017; Avand et al. 2021; Nkiaka and Okafor 2024). Despite the plethora of methods, hydrological models remain the most widely used approach probably because of their ability to explain physical processes to some extent (Addor and Melsen 2019). However, hydrological models require many parameters for calibration which may increase the uncertainty in the results (Nkiaka et al. 2018; Herrera et al. 2022; Wu et al. 2021). Furthermore, the application of hydrological models requires considerable input data including observed surface runoff, which is crucial for constraining the models, thus limiting their application in data-scarce regions (Nkiaka 2022). On the other hand, experimental methods involving paired catchment studies can take longer time and resources. Due to these challenges, the use of analytical methods to quantify the impact of climate variability and vegetation cover change on surface runoff is becoming increasingly popular (Hasan et al. 2018; Avand et al. 2021; Zhang et al. 2023). Analytical methods use mostly mathematical analysis based on the assumption that the basin water balance remains constant over a long period of time without significant changes in climate and basin characteristics (Dey and Mishra 2017; Zhang et al. 2023). Widely used analytical methods include the Elasticity concept (Liu et al. 2017; Tsai 2017), the Budyko framework (Gunkel and Lange 2017; Abera et al. 2019) and statistical techniques such as the partial least squares regression (PLSR) (Gebremicael et al. 2019; Zhou et al. 2021). The main advantage of analytical methods is that they do not require much input data to produce results that are useful in most hydrological applications (Hasan et al. 2018), making such methods well suited for data-scarce regions such as the Sahel (Gunkel and Lange 2017; Abera et al. 2019).

The present study focuses specifically on the Sahel region due to its high vulnerability to climate change and variability and other environmental stressors such as land degradation (Wendling et al. 2019). For example, previous studies found that the Sahel was particularly sensitive to climate variability and land degradation which led to the first "Sahel hydrological paradox". This was characterised by a significant increase in surface runoff despite a substantial decline in annual rainfall during the mega Sahel drought that lasted from the 1970s to mid-1990s (Descroix et al. 2009; Gal et al. 2017; Yonaba et al. 2021). Recent studies in the Sahel have shown a progressive recovery in rainfall (Sanogo et al. 2015; Gbohoui et al. 2021) and a general re-greening (Kaptué et al. 2015; Souverijns et al. 2020; Jiang et al. 2022). However, the re-greening of the Sahel has not led to a decline in surface runoff as expected which has been termed the second "Sahel hydrological paradox" observed from around the year 2000 (Descroix et al. 2018; Gbohoui et al. 2021; Yonaba et al. 2021). However, most studies reporting on these findings and wider hydrological processes in the region have focused on small experimental watersheds mostly around the central Sahel (Gal et al. 2017; Grippa et al. 2017; Wendling et al. 2019; Yonaba et al. 2021). To our knowledge, there is no study reporting on the "Sahel hydrological paradox" that covers all the watersheds located within the Sahelian belt from western to eastern Sahel. This is a key knowledge gap on the Sahelian hydrology that the present study intends to address.

The availability of long-term and high-resolution surface runoff data derived from water resources reanalysis (WRR) such as Famine Early Warning Systems Network (FEWS NET) Land Data Assimilation System FLDAS and other geospatial data including the fifth-generation atmospheric reanalysis of the European Centre for Medium-Range Weather Forecast (ERA5), Climate Hazards Group InfraRed Precipitation with Station data (CHIRPS) and normalised difference vegetative index (NDVI) used for monitoring vegetation cover change now makes this study feasible and extremely timely. However, the adoption of geospatial data for such studies requires careful validation (Dembélé et al. 2020a, 2020b; Nkiaka et al. 2022), to ensure that the results of the analyses are fit for purpose.

From the above, the objectives of this study are to: (1) analyse trends in annual surface runoff, climatic variables, and vegetation cover over a period of two decades (2000–2021), (2) identify the dominant climatic and environmental factors influencing surface runoff over the same period and, (3) quantify the impact of climate factors, soil moisture and vegetation cover on surface runoff across the Sahel over the same time period.

2 Study Area and Data

2.1 Study Area

Stretching from Senegal to Djibouti with a length of 8000 km, the Sahelian belt lies between latitude 12°N and 20°N and 20°W and 40°E. The estimated population living in the Sahel is about 150 million spread across parts of Burkina Faso, Chad, Eritrea, Mali, Mauritania, Niger, Nigeria, Senegal, and Sudan (Fig. 1). It is one of the largest water-limited and fragile ecosystems in the world; extremely vulnerable to the impacts of climate change and variability and prone to land degradation (Wendling et al. 2019; Mirzabaev et al. 2022). The population is mostly agrarian and depend on rain-fed agriculture and animal husbandry for livelihood, making them vulnerable to food insecurity due to erratic rainfall and poor soil quality (Jellason et al. 2021). The present study covers 45 watersheds (Table 1) nested within six major hydrological

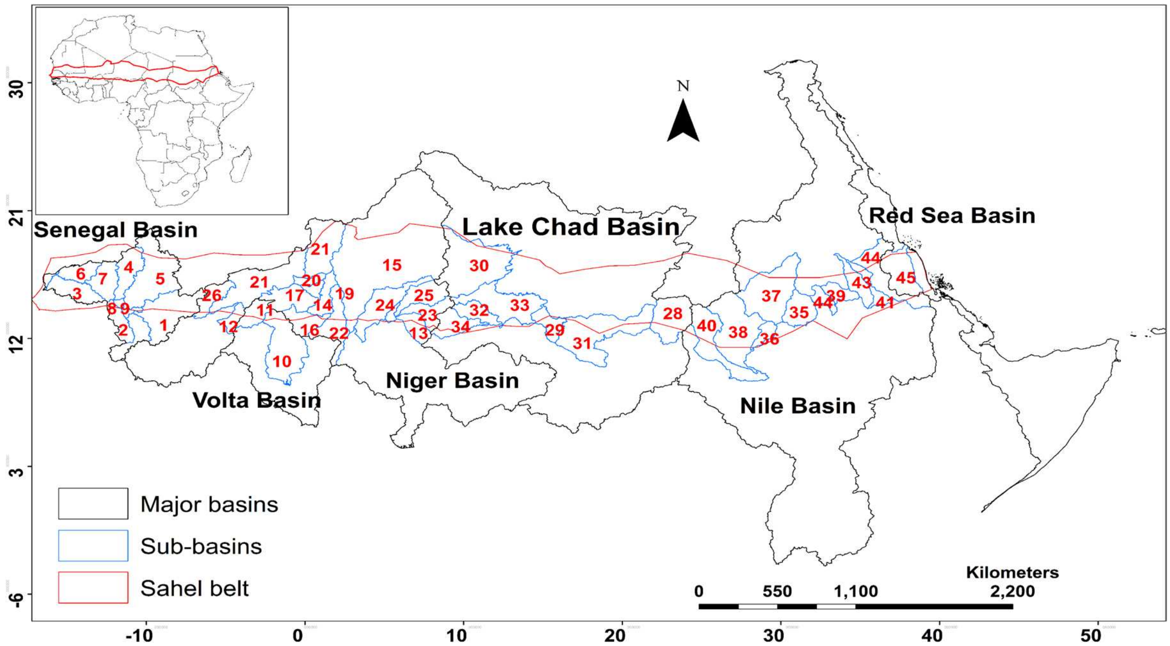

Fig. 1 Map of the study area showing the Sahel belt, major basins, and sub-basins. Sub-basins are numbered from left to right starting with the Senegal basin

basins including Senegal, Volta, Niger, Lake Chad, Nile, and Red Sea (Fig. 1). The sub-basins cover a total area of about 3,021,412 km^2 ranging in size from 4095 km^2 (Senegal 3) to 541,267 km^2 (Dallol Bosso) (Table 1). Shapefiles of the nested sub-basins were collected from HydroSHEDs which provides a seamless global coverage of consistently sized and hierarchically nested sub-basins at different scales using high-resolution Shuttle Radar Topographic Mission digital elevation model (Lehner and Grill 2013). Shapefiles from HydroSHEDs have been used extensively in several studies (Gebrechorkos et al. 2022; Odongo et al. 2023; Zhang et al. 2023).

2.2 Data

2.2.1 Climate Data

Precipitation data was obtained from CHIRPS at a spatial resolution of 0.05° × 0.05° and covers the period from 1981 to present at a daily timescale (Funk et al. 2015). CHIRPS has been validated e.g., (Abdourahamane 2021) and used in different studies in the Sahel e.g., (Elagib et al. 2021). Potential evapotranspiration (PET) data were obtained from ERA5 which is a reanalysis product providing global estimates of atmospheric and climatic variables at a spatial resolution of 0.25° from 1979 to present. ERA5 data has been used extensively for different studies in the Sahel e.g., (Dembélé et al. 2020a, 2020b; Elagib et al. 2021; Jiang et al. 2022).

2.2.2 Surface Runoff, Soil Moisture and Evapotranspiration Data

Due to a lack of long-term in situ data, we employed surface runoff, soil moisture (SM), and actual evapotranspiration (ET) data from FLDAS-Noah WRR which is a custom instance of the NASA Land Information System (LIS) framework (McNally et al. 2017). FLDAS-Noah is a land surface model (LSM) and the latest version of Noah used in FLDAS has a spatial resolution of 0.1° at monthly timescale. Surface runoff, and ET data from FLDAS-Noah have been validated in several basins in West Africa (Nkiaka et al. 2022). SM data used in this study range from 0–100 cm.

2.2.3 Vegetation Cover Data

Normalised Difference Vegetation Index (NDVI) data were used as a proxy for vegetation cover. The data came from Moderate Resolution Imaging Spectroradiometer (MODIS) satellite MOD13A1 V6 at a temporal resolution of 16 days and at 500 m spatial resolution available since 2000 (Didan 2015). NDVI data from MODIS have been

Table 1 Characteristics of the sub-basins located across the Sahel belt

Major Basin	Sub-basin	Number	Area (km^2)
Senegal	Bakoy	1	101,792
	Faleme	2	29,880
	Ferlo	3	45,131
	Karakoro	4	47,574
	Kolinbine	5	124,013
	Senegal 1	6	30,152
	Senegal 2	7	43,436
	Senegal 3	8	4,094
	Senegal 4	9	7,086
Volta	Nakanbe	10	110,851
	Sourou	11	31,072
Niger	Bani 1	12	18,610
	Bunsuru	13	31,043
	Dallol Maouri	14	71,197
	Dallol Bosso	15	541,267
	Faga	16	39,113
	Gorouol	17	53,944
	Niger 9	18	60,907
	Niger 10	19	31,167
	Niger 11	20	11,467
	Niger 12	21	12,352
	Niger 13	22	123,166
	N' kaba	23	38,787
	Rima	24	6,585
	Tarka	25	48,140
	Tchegue	26	32,872
	Tilemsi	27	87,033
Lake Chad	Bahr Azum	28	77,960
	Bouluo	29	31,407
	Dillia	30	162,385
	Fitri	31	143,576
	Komadugu Yobe 1	32	33,318
	Komadugu Yobe 2	33	97,568
	Koramas	34	43,751
Nile	Abu Hut	35	45,971
	Al Ghallah	36	17,948
	Al Malik	37	125,049
	Bandah	38	129,875
	Blue Nile 1	39	23,014
	Gelha	40	90,900
	Nahr Atbarah 1	41	25,088
	Mereb Wenz	42	73,113
	Wadi Atshan	43	33,722
	White Nile 1	44	17,690
Red Sea	Nahr al Qash	45	66,346

used in many studies in West Africa e.g., (Zoungrana et al. 2018; Ibrahim et al. 2021; Jiang et al. 2022).

3 Methods

3.1 Gridded Data Aggregation

CHIRPS, ERA5, FLDAS-Noah and NDVI data were aggregated to annual timescale to correspond to the timescale of our analyses and downloaded at their respective native spatial resolutions using the Climate Engine research App [https://app.climateengine.com] (Huntington et al. 2017). Climate engine is an open data platform used for accessing, processing, visualizing, and analysing earth observation datasets via a simple web connection, thereby overcoming the computational burden of big data, and providing the ability to customise data download (Huntington et al. 2017). Sub-basins shapefiles may be uploaded to Climate Engine directly from a computer folder or using the Google Earth Engine interface.

3.2 Annual Surface Runoff Coefficient

Annual runoff coefficient defined as the ratio of annual surface runoff to precipitation was estimated using the following equation:

$$C = {}^{Q}/_{P} \tag{1}$$

where C is the runoff coefficient, Q is surface runoff and P is precipitation.

3.3 Trend and Correlation Analyses

The non-parametric Mann–Kendall (Mann 1945; Kendall 1970) test was used for trend analysis and significance while and Sen's slope estimator (Sen 1968) was used to quantify trend magnitude from 2000 to 2021. The Mann–Kendall trend test and Sen slope estimators are widely used to analyse trends and magnitudes in hydroclimatic timeseries. Trend analyses were conducted at the 5% significance level.

3.4 Factors Influencing Surface Runoff

Different statistical techniques are used to establish the relationship between the dependent variable (surface runoff) and the independent variables (precipitation, PET, SM and NDVI) including multivariable linear regression (MLR) and partial least squares regression (PLSR). Different statistical techniques are used to explore the strength and complement the weaknesses of each technique. The advantage of using PLSR is that it can mitigate the effects of multi-collinearity and interactions among variables and can also maximise the covariance between two hydrological quantities (Kaushik et al. 2023).

MLR analysis was used to establish the relationship between the rate of change in surface runoff (dependent variable) and the rate of change in independent variables in order to determine which of the independent variables exerts stronger influence on surface runoff. To achieve this, we first standardized the variables by dividing the variable anomalies by the standard deviation of that variable. The relationship between the variables was then estimated using multivariable regression statistics at 5% significance level using Eq. (2). The relative contribution of the rate of change in each independent variable to the rate of change in runoff was estimated from the multivariate regression coefficients using Eq. (3).

$$Y = aX_1 + bX_2 + cX_3 + dX_4 \tag{2}$$

$$r_x = \frac{|a|}{|a| + |b| + |c| + |d|} \tag{3}$$

where Y is the standardized dependent variable (runoff), $X1$, X_2, X_3, and X_4 are standardized independent variables for precipitation, PET, SM and NDVI; r_x is the relative sensitivity of surface runoff to these factors while *a, b, c, &* *d* are the regression coefficients.

Lastly, variable importance in projection (VIP) from PLSR was also used to evaluate the influence of each independent variable on dependent variable considering the collinearity among the variables. To achieve this, the independent variables data matrices are statistically rotated such that only relevant PLSR components are used in predicting the change in the dependent variable (Kaushik et al. 2023). The VIP has been used in different studies e.g., to understand the influence of climate and environmental variables on ET in China (Wu et al. 2023), the impact of land use change on streamflow in Ethiopia (Gebremicael et al. 2019) and the impact of soil moisture-atmosphere feedbacks in mitigating declining water availability in global drylands (Zhou et al. 2021). VIP scores from PLSR analysis are estimated using following equation:

$$VIP = \sqrt{\frac{\sum_{f=1}^{F} w_{jf}^2 \cdot SSY_f \cdot J}{SSY_{total} \cdot J}} \tag{4}$$

where W_{jf} is the weight value for j variable and f component, and SSY_f is the sum of squares of explained variance for the f^{th} component and J number of independent variables in the data matrix. SSY_{total} is the total sum of squares explained of the dependent variable, and F is the total number of components. $W^2{}_{jf}$ is the importance of each j^{th} variable in f^{th} component, VIP is a measure of the global contribution of j variable in the PLSR model. As a rule of thumb, $\text{VIP} > 1$ is statistically significant to explain the dependent variables as used in different studies (Gebremicael et al. 2019; Wu et al. 2023).

3.5 Elasticity Concept

The elasticity concept is used to quantify the effects of climatic factors, SM and NDVI on surface runoff. The elasticity concept is useful for quantifying how a relative change in one variable affects the other variable (Tan et al. 2020). The extensive use of the elasticity concept in hydrology may be attributed to its clear physical meaning and simple formulation (Sankarasubramanian et al. 2001; Khan et al. 2022). Since its original formulation, several other elasticity models have been proposed. For example, Sankarasubramanian et al. (2001) introduced the non-parametric model based on observed long-term hydrometeorological data, Zheng et al. (2009) introduced the least square elasticity model and the multivariable double logarithm and multivariable transformation analyses models were proposed by (Tsai 2017). The least squares elasticity model proposed by Zheng et al. (2009) was adopted in this study because it can overcome the problem associated with small sample size. The model is expressed as:

$$\varepsilon = \frac{\overline{X}}{\overline{Q}} \cdot \frac{\sum\left(X_i - \overline{X}\right)\left(Q_i - \overline{Q}\right)}{\sum\left(X_i - \overline{X}\right)^2} = \rho_{X,Q} \cdot {C_Q}/{C_X} \tag{5}$$

where Q is the annual surface runoff and X represent the annual climatic or environmental variable (precipitation, PET, SM and NDVI) and $\overline{X}$ and $\overline{Q}$ represent the multiyear annual mean climatic/environmental variable and surface runoff values respectively. $\rho_{X,Q}$ is the correlation coefficient between the climatic variable and surface runoff and C_X and C_Q are the coefficients of variation of climatic variable and surface runoff, respectively.

3.6 Budyko Framework

The Budyko framework (Budyko 1974) is used to understand how climatic factors and catchment characteristics affect the partitioning of precipitation into runoff and evapotranspiration. The framework is based on the long-term water balance and assumes that water and energy are the dominant factors that control how precipitation is partitioned between surface runoff and ET over a long time period. Under hydrological steady state conditions, the partitioning of precipitation into surface runoff and ET in watersheds is assumed to follow the Budyko curve. If watersheds are assumed to follow the Budyko curve, it is possible to account for reasons why some watersheds deviate from their Budyko curve (Wamucii et al. 2021). Watershed deviation from the Budyko curve may be due to changes in climatic conditions characterized by changes in evaporative and aridity indices which may translate to vertical and horizontal shifts respectively within the Budyko space (Gbohoui et al. 2021).

Several analytical equations of the Budyko curve are available in the literature. This study adopts the one parameter Fu's equation which has been applied extensively in Africa (Li et al. 2013; Abera et al. 2019; Wamucii et al. 2021). In addition, a sensitivity analysis carried out in the Nakanbe basin using different Budyko models showed that the Fu model was suitable in dryland areas (Gbohoui et al. 2021). Moreover, unlike the non-parametric Budyko model that is applicable to large spatial domains and at longer timescales (> 10,000, > 1 year), parametric models are applicable to a wide range of temporal and spatial scales (Donohue et al. 2007). The Fu's equation relates the aridity index (PET/P) (x-axis) to the evaporative index (ET/P) (y-axis) using a dimensionless empirical parameter (ω) that determines the shape of the curve and also accounts for the impact of landscape characteristics such as soil, topography, vegetation and climate variability on water and energy balance (Li et al. 2013). The Fu's equation is given as:

$$\frac{ET}{P} = 1 + \frac{PET}{P} - \left[1 + \left(\frac{PET}{P}\right)^{\omega}\right]^{\frac{1}{\omega}} \quad (6)$$

where *P, ET,* and *PET* are precipitation, actual evapotranspiration, and potential evapotranspiration respectively. Despite its wide application in hydrology, the Budyko framework has been criticized for not been reflective of the dynamic behaviour of individual watersheds (Reaver et al. 2022).

Different techniques have been used to estimate the *ω* parameter. For example, Li et al. (2013), Abera et al. (2019) and Gbohoui et al. (2021) adopted a curve fitting procedure that minimizes the mean square error between the simulated and observed evaporative index. Other studies e.g., Creed et al. (2014) adopted fixed values to represent different land cover classes. This study adopts the curve fitting technique due to its ability to minimize the mean square error between the simulated and observed evaporative index. As such, the values of the *ω* parameter in each watershed are estimated by forcing the Budyko-type model of Fu (1981) with values of P, PET, and ET over the period 2000–2021. The curve fitting procedure was implemented using the following objective function:

$$obj = min \sum \left[\frac{ET}{P} - \left[1 + \frac{PET}{P} - \left[1 + \left(\frac{PET}{P}\right)^{\omega}\right]^{\frac{1}{\omega}}\right]\right]^2 \quad (7)$$

To establish the relationship between landscape characteristics and vegetation cover, a scatterplot was created between the NDVI values and the optimized ω for all the watersheds and a linear regression model fitted between the two variables.

Lastly, the *ω* values obtained were compared with Eqs. (8) developed by Li et al. (2013) for global river basins and Eq. (9) developed by Gbohoui et al. (2021) for several nested watersheds in the Nakanbe river basin located slightly to the south of the Sahel belt.

$$\omega = 2.36M + 1.16 \quad (8)$$

$$\omega = 6.27M + 0.98 \quad (9)$$

4 Results

4.1 Spatial Variability in Annual Hydroclimatic and Vegetation Variables

Analyses show strong spatial heterogeneities for annual precipitation across the different sub-basins varying from 1021 mm/year in the Faleme sub-basin (Senegal basin) to 75 mm/year in the Dillia sub-basin Lake Chad Basin (LCB) (Fig. 2a).

PET also varies strongly across the sub-basins ranging from 1800 to 2100 mm/year, while SM follows the same pattern as annual precipitation (Fig. 2b, c). Annual NDVI equally follows a similar pattern as precipitation with sub-basins in the southern portion of the Sahel belt where precipitation is higher showing higher NDVI values. Annual runoff in most sub-basins lies between 3 and 20 mm/year and only exceeds 80 mm/year in one sub-basin located in the Senegal basin (Fig. 2e). Annual runoff coefficient also shows strong spatial variability across the Sahel (Fig. 2f).

4.2 Trends in Annual Hydroclimatic and Vegetation Conditions

Annual precipitation shows statistically significant increasing trends in more than 80% of the watersheds, however, there a few watersheds located in the Senegal and Niger basins with statistically significant decreasing trends (Fig. 3a).

Trends in annual PET also show mixed results with both statistically significant increasing and decreasing trends

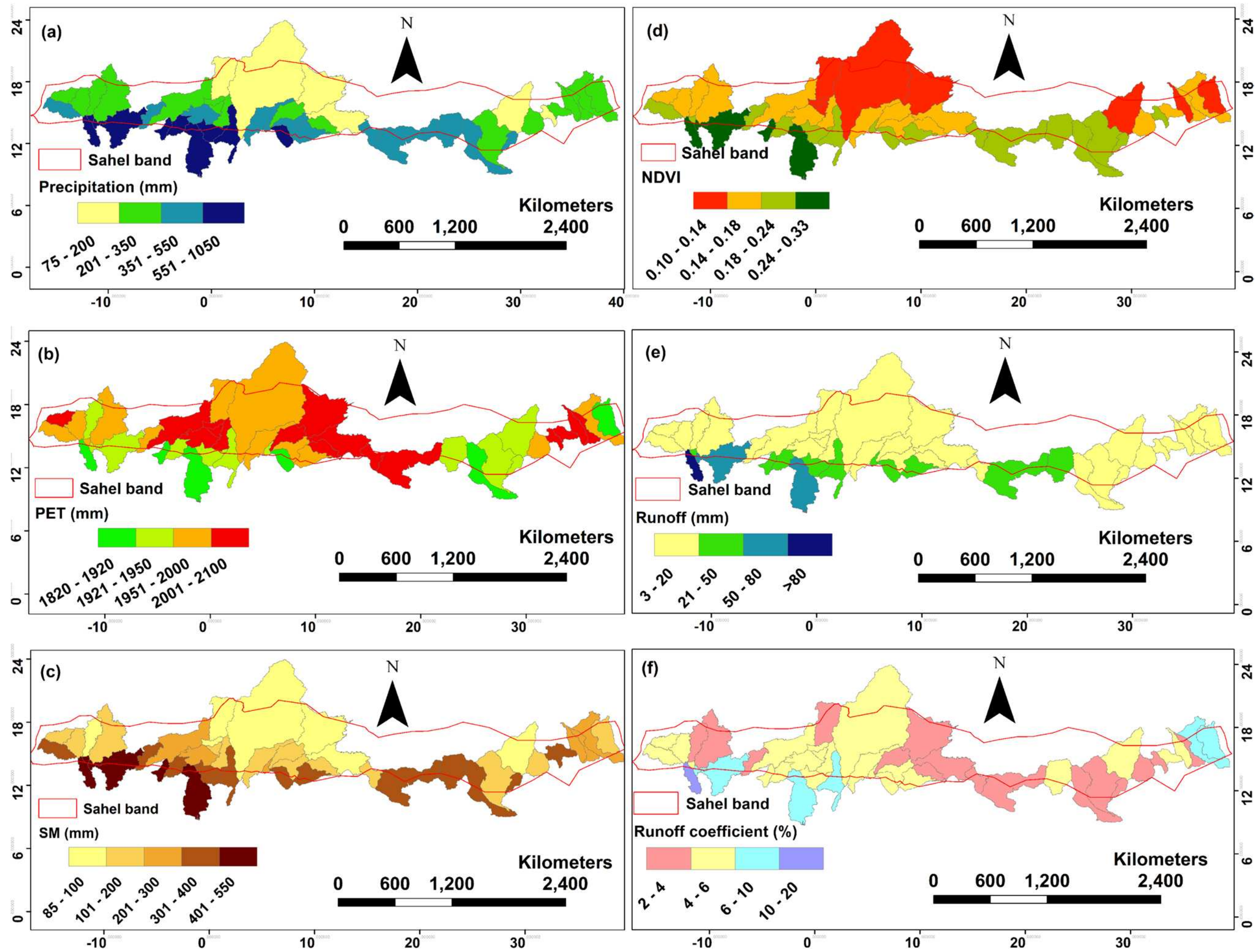

Fig. 2 Spatial variability in mean annual **a** precipitation, **b** PET, **c** soil moisture, **d** NDVI, **e** runoff and **f** runoff coefficient over the period (2000–2021)

across the study area. Higher trend magnitudes (> 3 mm/year) occur mostly around the central and western Sahel while most watersheds in the eastern Sahel (Lake Chad and Nile basins) show decreasing trends in annual PET (– 1.5 mm/year) (Fig. 3b). Analyses also show statistically significant increasing trends in SM around the central, western and parts of the eastern Sahel (Fig. 3c). Annual NDVI also show statistically increasing trends across the study area with most sub-basins in the south displaying higher trend magnitudes. Statistically significant trends in annual runoff are also observed across the study area with Faleme sub-basin in the Senegal basin showing the highest magnitude in annual runoff (> 10 mm/year) (Fig. 3e). There are also statistically significant increasing trends in annual surface runoff coefficient across all sub-basins ranging from 2 to 4.5% per year. However, trend magnitudes vary across the study area with most nested sub-basins in the Lake Chad Basin showing the highest magnitude in annual runoff coefficient (> 4.5% per year) (Fig. 3f).

4.3 Using Statistical Methods to Identify the Factors Influencing Surface Runoff

Results of the statistical analyses are available in Table 2. Analyses using MLR show that the independent variables contribute about 62% of the observed variance in surface runoff with relative contributions (weight) of 62%, 17%, 2% and 19% respectively for precipitation, PET, SM and NDVI (Table 2). On the other hand, statistical analyses using PLSR show that precipitation and NDVI are the dominant factors influencing surface runoff given that their respective VIP scores are both greater than 1.0 (Table 2).

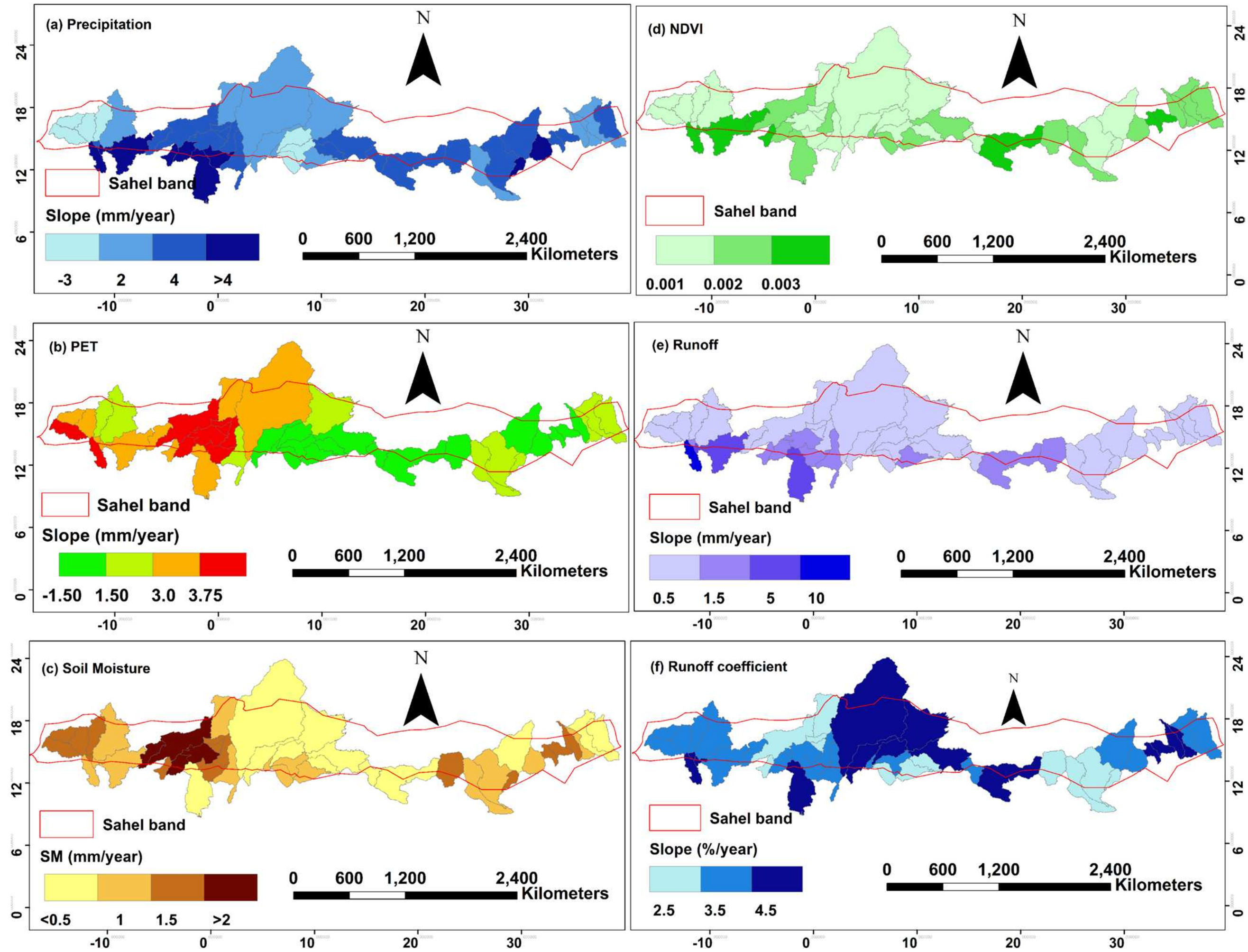

Fig. 3 Trends in annual **a** precipitation, **b** PET, **c** soil moisture, **d** NDVI, **e** runoff and **f** runoff coefficient over 2000–2021

Table 2 Results of analyses for change in annual runoff

Variable	MLR		PLSR	
	Relative weight	Variance explained (%)	Variance explained (%)	VIP
Precipitation	0.29	61.66	38.68	1.31
PET	0.08	16.79	22.85	0.67
SM	0.01	2.03	8.11	0.63
NDVI	0.09	19.52	30.36	1.21

4.4 Quantifying the Impact of Climate Variability and vegetation Cover on Surface Runoff Using the Elasticity Concept

The elasticity coefficients are used to indicate how a change in an independent variable will result to a corresponding change in the dependent variable. The mean elasticity coefficients of the independent variables (precipitation, PET, SM and NDVI) to annual surface runoff change over the period 2000–2021 are shown in Fig. 4. Analyses show that an increase in precipitation, SM and NDVI will lead to a corresponding increase in surface runoff across all the watersheds as shown by their mean positive elasticity coefficients (Fig. 4a–d). On the contrary, an increase in PET will lead to a decline in surface runoff in most watersheds as shown by its mean negative elasticity coefficient (Fig. 4b). However, PET influences surface runoff to a greater extent than precipitation due to its higher mean elasticity coefficient (-6.07). The elasticity coefficients of the independent variables are in the range 1.10 to 4.80, −19.80 to 24.21, 0.11 to 8.25 and 0.02 to 8.38 with mean elasticities of 2.19, −6.07, 2.61, and 4.54 for precipitation, PET, SM and NDVI respectively. This suggests that a 10% increase in precipitation, SM and NDVI will increase surface runoff by approximately 22%, 26% and 45% respectively while 10% increase in PET will decrease surface runoff by about 61%.

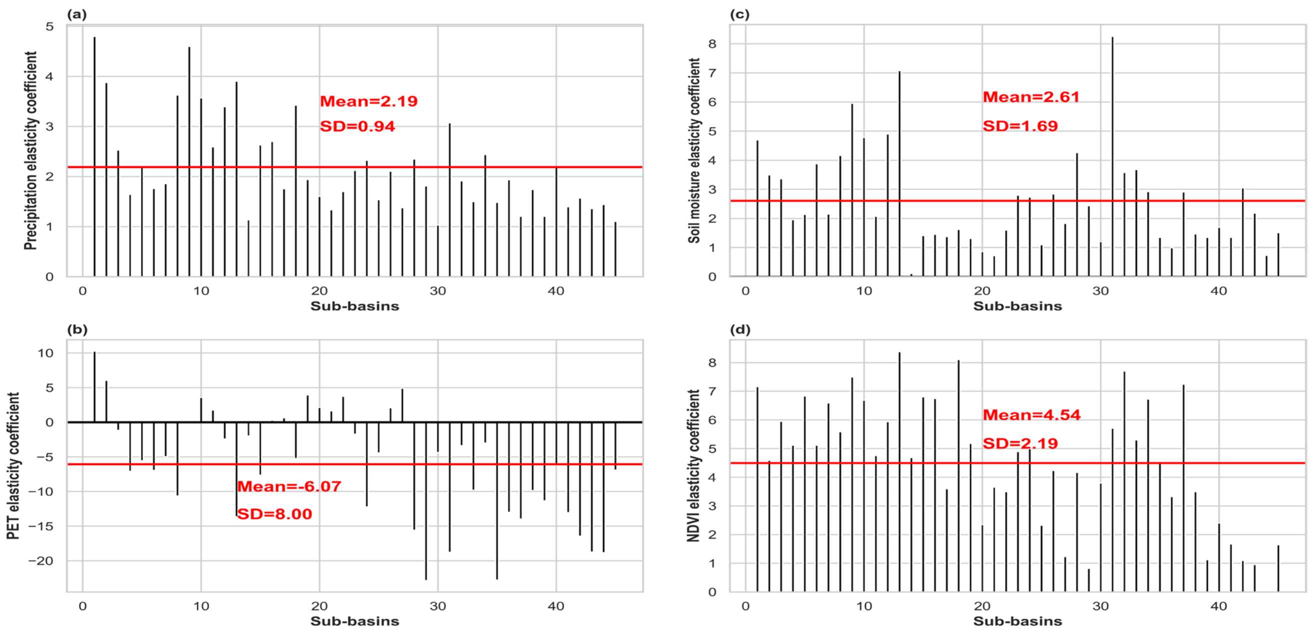

Fig. 4 Distribution of elasticity coefficients of runoff across the different watershed **a** precipitation, **b** PET, **c** soil moisture, and **d** NDVI. Each vertical line represents a sub-basin, the red horizontal line is the mean value for all the watershed and SD: standard deviation

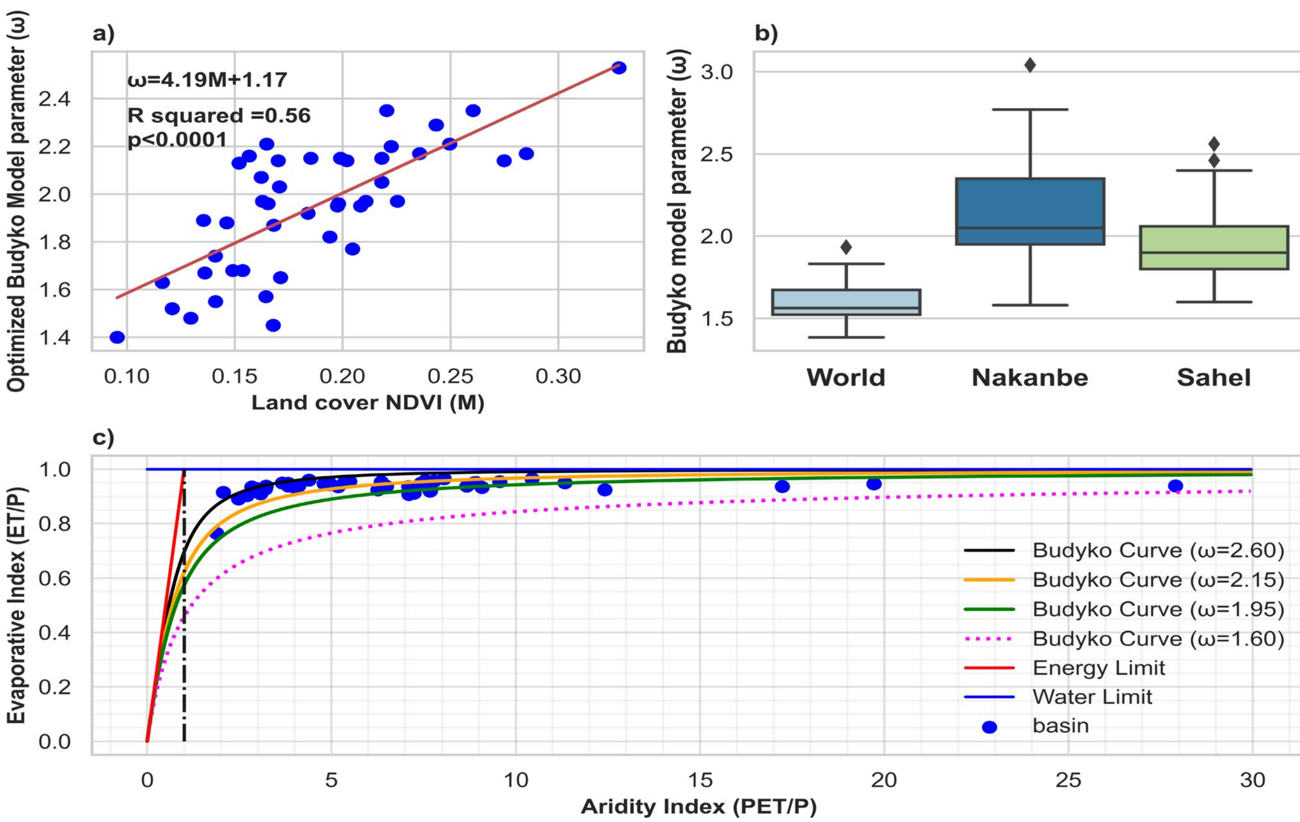

Fig. 5 **a** relationship between optimized Fu model parameter (ω) and land cover conditions (M), **b** boxplot showing optimized Fu model parameter (ω) and values obtained from Eq. (8), (9) & (10) and **c** partitioning of precipitation into runoff and ET within the Budyko space using the one parameter Fu model. (Each blue circle in the figure represents a watershed). The red line in Fig. 5a represents the linear regression between ω and M

4.5 The Budyko Framework

Specific values of ω for all the 45 watersheds are obtained using a curve fitting procedure in Eq. (7). Figure 5a shows that long-term mean land cover conditions (M) correlates moderately ($R^2 = 0.56$, *p-value* < 0.0001) with the optimized ω values at the 5% significance level. The relationship between M and the ω values is a linear regression equation in Fig. 5a given as:

$$\omega = 4.19 \times M + 1.17 \tag{10}$$

Next, ω values are estimated for all the watersheds by substituting long-term mean land cover conditions (M) in Eqs. (8), (9) & (10). Figure 5b, shows that the optimized ω values obtained in this study using Eq. (10) are slightly higher than those obtained using the Eq. (8) for global basins but lower than those obtained from Eq. (9) in the Nakanbe basin located slightly to the south of the Sahelian belt.

Figure 5c shows the partitioning of precipitation into runoff and ET within the Budyko space for the period 2000–2021. All watersheds are mapped into high aridity space with AI > 2 (Fig. 5c), which reflects the characteristics of the Sahel as an arid environment. It can also be observed using a mean ω value of 1.95 obtained in this study, it is possible to capture the partitioning of precipitation into runoff and ET in most watersheds including those mapped into both high and low aridity and evaporative indices space (Fig. 5c).

5 Discussion

Generally, analyses show that the different watersheds exhibit trends of varying magnitudes over the study period (200–2021).

5.1 Hydroclimatic Trends

The spatial heterogeneity in precipitation across the Sahel may be attributed to several factors such as the seasonal migration of the intertropical convergence zone (ITCZ) which is partly responsible for rainfall distribution in the Sahel (Lebel and Ali 2009). Precipitation distribution across the Sahel is also partly controlled by mesoscale convective systems (Taylor et al. 2017; Vizy and Cook 2022). Increasing trends in climatic variables follow similar patterns obtained in previous studies across the Sahel e.g., precipitation (Sanogo et al. 2015; Gbohoui et al. 2021) and PET (Ndiaye et al. 2020). Increasing trends in vegetation cover are also consistent with results from several studies (Kaptué et al. 2015; Souverijns et al. 2020; Jiang et al. 2022). This may be attributed to increasing precipitation patterns in the region. Results of trend analysis are consistent with those of other studies showing increasing trends in runoff coefficient and runoff volumes despite increasing trends in vegetation cover (Descroix et al. 2018; Gbohoui et al. 2021; Yonaba et al. 2021).

Increasing runoff volumes have several implications on livelihoods in the Sahel such as increasing flooding risk which could lead to health risk, water, and food security. For example, recent studies have reported an increasing trend in flood incidences across the region (Tazen et al. 2019; Elagib et al. 2021; Miller et al. 2022). Flooding may also increase the risk of vector borne diseases such as Malaria and Chikungunya (Jambou et al. 2022; Thomas et al. 2022). It may also contribute to reduce agricultural yield due to water stagnation in cultivated fields, thereby exacerbating food insecurity (Daku et al. 2022). Future research may seek to investigate how and to what extent ecological restoration efforts through afforestation such as the great green wall may affect flood peaks in the Sahel.

5.2 Factors Influencing Surface Runoff

MLR and PLSR both show that there is a strong coupled relationship between surface runoff, precipitation, and vegetation cover in the Sahel. Whilst increasing vegetation cover was expected to reduce surface runoff volumes as reported in several studies (Buechel et al. 2022; Liu et al. 2022; Ricciardi et al. 2022), the two variables are increasing concurrently in the Sahel, and this has been termed the second "Sahel hydrological paradox". The second "Sahel hydrological paradox" has still been attributed to the extensive land degradation that occurred during the mega drought from the 1970s to the mid-1990s, reducing soil water holding capacity and root depth while increasing soil crusting, thereby reducing soil infiltration capacity and enhancing surface runoff generation (Descroix et al. 2018). Other studies attribute increasing surface runoff to changes in soil properties and the non-recovery of tiger bush in some areas (Dardel et al. 2014; Gal et al. 2017). Descroix et al. (2018) argues that the current re-greening of the Sahel may not have reached a minimum threshold that can off-set extensive land degradation to enhance infiltration and reduce surface runoff, hence the continuous increase in surface runoff. Even though substantial research has been conducted to explain the "Sahel hydrological paradox", its causes are still strongly debated e.g., (Descroix et al. 2018; Yonaba et al. 2023). As such, additional research is needed to shed more light on the "Sahel hydrological paradox".

Considering that the independent variables explained only about 62% of total variance in surface runoff, this suggest that there may be other factors such as topography and other physical attributes of the watersheds exerting additional influence on surface runoff. Therefore, more studies are needed to identify other factors influencing surface runoff in the Sahel. Whilst previous studies investigating the relationship between climate and vegetation cover on surface runoff in the Sahel are limited to a few experimental watersheds around the central Sahel, the present study covers the whole Sahelian belt from western to eastern Sahel thereby providing additional evidence on the second “Sahel hydrological paradox”.

5.3 Quantifying Surface Runoff Change

The elasticity concept was used to understand how a change in each independent variable will affect the dependent variable. Results from analyses suggest that PET has a greater influence on surface runoff, followed by vegetation cover (NDVI), SM and precipitation in descending order. However, an increase in NDVI has a higher mean positive elasticity coefficient than precipitation and soil moisture. This suggest that the same amount of increase in NDVI may lead to a two-fold increase in surface runoff while the same amount of increase in precipitation and SM will only lead to a one-fold increase in surface runoff. On the other hand, the same amount of increase in PET may lead to a three-fold decline in surface runoff. Results from our analyses are consistent with those from a previous study in the region (Yonaba et al. 2021). A recent study covering the global domain has also shown that an increase in PET has a strong negative effect on annual runoff (Zhang et al. 2023). The elasticity coefficients suggest that a 10% increase in precipitation, SM and NDVI will increase runoff by a combine total of 93% while a 10% increase in PET will reduce runoff by 61%.

5.4 Climate-Catchment Interaction

In this study, change in environmental factor is analysed using the ω parameter in the Fu equation. The Fu equation was used to reveal how the interaction between climate and catchment characteristics influence the partitioning of precipitation into surface runoff and ET. Analyses show that all the watersheds were mapped into the high aridity space within the Budyko curve which reflects the characteristics of the Sahel as an arid region. As such, ET in the Sahel may only be limited by water supply than by energy. The mean omega value obtained in the Sahel is 1.95 which is less than the default Budyko-Fu parameter ($\omega = 2.6$). The difference between ω values obtained in the Sahel and the default value may be attributed to differences in watershed sizes considering that watersheds characteristics play a key role in the partitioning of precipitation in smaller watersheds while climate play a greater role in larger watersheds (Kingston et al. 2020). It could also be due to the climatology of the different study areas in both studies.

Next, we compare the value of the regression coefficient obtained in this study (4.19) with the value obtained in global basins (2.36). The results suggest that for the same change in M, the ω in Sahel will vary by two-folds from that estimated by Eq. 8 for global basins. On the contrary for the same change in M, the ω in the Sahel will vary by about 67% (33% less) than that estimated by Eq. 9 in the Nakanbe basin. The difference between the value obtained in this study and the Nakanbe basin may be attributed to higher NDVI values (mean NDVI = 0.26) in the Nakanbe basin compared to the Sahel (mean NDVI = 0.19). Analyses also show a statistically significant relationship between land cover conditions (M) and the optimized ω parameter which represents both landscape characteristics and climate conditions which is consistent with results from another study in the region (Gbohoui et al. 2021). This suggest that increasing vegetation cover may lead to a corresponding positive change in landscape characteristics in the Sahel. Understanding how vegetation cover influences landscape characteristics may be critical for adopting environmental management policies such as ecological restoration.

Generally, results from analytical methods conducted in this study are comparable to results obtained using hydrological models in the Sahel (Gal et al. 2017; Descroix et al. 2018; Wendling et al. 2019; Yonaba et al. 2021). This therefore suggest that analytical methods are a promising approach for understanding the effects of climatic factors and vegetation cover change on surface hydrology in data-scarce regions.

5.5 Limitations of the Study

We wish to highlight that even though the data used in this study was obtained from different sources, all the datasets have been validated and used extensively in other studies in the Sahel. Despite their extensive validation and use in the region, we acknowledge that the data are not exempt from inherent biases which may influence our results. We also wish to highlight that using surface runoff data generated from other WRR models may not yield the same results due to the differences in model parameters and input data used in generating the surface fluxes. Furthermore, the Budyko model which is used in this study assumes that the watersheds are under hydrological steady state conditions over the study period. This implies that the partitioning of precipitation into surface runoff and ET is not influenced by changes in groundwater storage and other catchment characteristics which may not be true. In fact, several studies e.g., (Condon and Maxwell 2017; Mianabadi et al. 2020; Reaver et al. 2022) have shown that the dynamic nature of watersheds including changes in water storage and inter-basin groundwater flow and changes in catchment characteristics may lead to shifts in the Budyko relationships. We consider these issues as some of the flaws in our study and therefore, wish to remind readers to interpret our results with caution.

6 Conclusions

The aim of this study was to quantify the impact of climatic factors, SM and vegetation cover change on surface runoff in 45 nested watersheds in the Sahel over a period of two decades 2000–2021 using analytical methods (elasticity concept, the Budyko framework and empirical statistics) along with geospatial data. Analyses using MLR and PLSR show that precipitation and NDVI are the dominant factors influencing surface runoff in the Sahel. Mean elasticity coefficients for precipitation, PET, SM and NDVI are 2.19, −6.07, 2.61, and 4.54 respectively. This suggest that a 10% increase in precipitation, SM and NDVI will increase runoff by a combined total of 93% while a 10% increase in PET will reduce runoff by about 61%. Analyses further reveal statistically significant ($R^2 = 0.56$, *p-value* < 0.0001) relationship between land cover conditions (M) and optimized ω parameter representing landscape characteristics and climate variability. The partitioning of precipitation into runoff and ET using the Fu equation shows that the ω parameter value (1.95) obtained in this study can capture the long-term water and energy balance in most watersheds compared to the default parameter (2.6) from the original Budyko-Fu model. Results from this study using analytical methods are comparable to modelling results in the region. This suggests that analytical methods may be used for assessing the effects of climatic factors, SM, and vegetation cover change on surface runoff in data-scarce regions. The present study improves our understanding of the climate-vegetation-runoff system in the Sahel and may be used to support climate adaptation and ecological restoration efforts in the Sahel such as the Great Green Wall Initiative.

7 Open Research

All data used to perform the analyses reported in this paper are freely available for download through the Climate Engine Research App at https://app.climateengine.com. (Last accessed: 18th October 2023 using a customized users' account).

Shapefiles for the major basins and their nested sub-basins are available from www.hydrosheds.org/hydrosheds-v2.

Author Contributions Elias Nkiaka: Conceptualization, Data Curation, Methodology, Investigation, Resources, Writing- Review & editing, Funding acquisition. Robert G. Bryant: Methodology, Investigation, Writing- Review & editing. Moctar Dembélé: Investigation, Writing-Review & editing.

Funding The first author was funded by the Leverhulme Trust Early Career Fellowship-Award Number ECF–097–2020.

Declarations

Conflict of Interest The authors declare that they have no conflict of interest.

References

Abdourahamane ZS (2021) Evaluation of fine resolution gridded rainfall datasets over a dense network of rain gauges in Niger. Atmos Res 252:105459

Abera W, Tamene L, Abegaz A, Solomon D (2019) Understanding climate and land surface changes impact on water resources using Budyko framework and remote sensing data in Ethiopia. J Arid Environ 167:56–64

Addor N, Melsen L (2019) Legacy, rather than adequacy, drives the selection of hydrological models. Water Resour Res 55:378–390

Avand M, Moradi H, Lasboyee MR (2021) Using machine learning models, remote sensing, and GIS to investigate the effects of changing climates and land uses on flood probability. J Hydrol 595:125663

Baggio G, Qadir M, Smakhtin V (2021) Freshwater availability status across countries for human and ecosystem needs. Sci Total Environ 792:148230

Budyko M (1974) Climate and life International geophysics series, 18. Academic New York.

Buechel M, Slater L, Dadson S (2022) Hydrological impact of widespread afforestation in Great Britain using a large ensemble of modelled scenarios. Commun Earth Environ 3:1–10

Condon LE, Maxwell RM (2017) Systematic shifts in Budyko relationships caused by groundwater storage changes. Hydrol Earth Syst Sci 21:1117–1135

Creed IF, Spargo AT, Jones JA, Buttle JM, Adams MB, Beall FD, Elder K (2014) Changing forest water yields in response to climate warming: results from long-term experimental watershed sites across North America. Glob Change Biol 20:3191–3208

Daku EK, Salack S, Worou ON, Ogunjobi K (2022) Maize response to temporary floods under ambient on-farm conditions of the West African Sahel. Environ Res Commun 4:045004

Dardel C, Kergoat L, Hiernaux P, Grippa M, Mougin E, Ciais P, Nguyen C-C (2014) Rain-use-efficiency: what it tells us about the conflicting Sahel greening and Sahelian paradox. Remote Sens 6:3446–3474

Dembélé M, Ceperley N, Zwart SJ, Salvadore E, Mariethoz G, Schaefli B (2020a) Potential of satellite and reanalysis evaporation

datasets for hydrological modelling under various model calibration strategies. Adv Water Resour 143:103667
Dembélé M, Schaefli B, van de Giesen N, Mariéthoz G (2020b) Suitability of 17 gridded rainfall and temperature datasets for large-scale hydrological modelling in West Africa. Hydrol Earth Syst Sci 24:5379–5406
Dembélé M, Vrac M, Ceperley N, Zwart SJ, Larsen J, Dadson SJ, Schaefli B (2022) Contrasting changes in hydrological processes of the Volta river basin under global warming. Hydrol Earth Syst Sci 26:1481–1506
Descroix L, Mahé G, Lebel T, Favreau G, Galle S, Gautier E, Cappelaere B (2009) Spatio-temporal variability of hydrological regimes around the boundaries between Sahelian and Sudanian areas of West Africa: A synthesis. J Hydrol 375:90–102
Descroix L, Guichard F, Grippa M, Lambert LA, Panthou G, Mahé G, Kergoat L (2018) Evolution of surface hydrology in the Sahelo-Sudanian strip: An updated review. Water 10:748
Dey P, Mishra A (2017) Separating the impacts of climate change and human activities on streamflow: A review of methodologies and critical assumptions. J Hydrol 548:278–290
Didan, K. (2015). MOD13A1 MODIS/Terra Vegetation Indices 16-Day L3 Global 500m SIN Grid V006. *NASA EOSDIS Land Processes DAAC,* 10
Donohue R, Roderick M, McVicar TR (2007) On the importance of including vegetation dynamics in Budyko's hydrological model. Hydrol Earth Syst Sci 11:983–995
Ebodé VB, Dzana JG, Nkiaka E, Nnomo BN, Braun JJ, Riotte J (2022) Effects of climate and anthropogenic changes on current and future variability in flows in the So'o River Basin (south of Cameroon). Hydrol Res 53:1203–1220
Elagib NA, Al Zayed IS, Saad SAG, Mahmood MI, Basheer M, Fink AH (2021) Debilitating floods in the Sahel are becoming frequent. J Hydrol 599:126362
Fu B (1981) On the calculation of the evaporation from land surface. Sci Atmos Sin 5:23–31
Funk C, Peterson P, Landsfeld M, Pedreros D, Verdin J, Shukla S, Hoell A (2015) The climate hazards infrared precipitation with stations—a new environmental record for monitoring extremes. Scientific Data 2:1–21
Gal L, Grippa M, Hiernaux P, Pons L, Kergoat L (2017) The paradoxical evolution of runoff in the pastoral Sahel: analysis of the hydrological changes over the Agoufou watershed (Mali) using the KINEROS-2 model. Hydrol Earth Syst Sci 21:4591–4613
Gbohoui YP, Paturel J-E, Tazen F, Mounirou LA, Yonaba R, Karambiri H, Yacouba H (2021) Impacts of climate and environmental changes on water resources: A multi-scale study based on Nakanbé nested watersheds in West African Sahel. Journal of Hydrology: Regional Studies 35:100828
Gebrechorkos SH, Pan M, Lin P, Anghileri D, Forsythe N, Pritchard DMW, Sheffield J (2022) Variability and changes in hydrological drought in the Volta Basin, West Africa. J Hydrol: Reg Stud 42:101143
Gebremicael T, Mohamed Y, Van der Zaag P (2019) Attributing the hydrological impact of different land use types and their long-term dynamics through combining parsimonious hydrological modelling, alteration analysis and PLSR analysis. Sci Total Environ 660:1155–1167
Greve P, Kahil T, Mochizuki J, Schinko T, Satoh Y, Burek P, Langan S (2018) Global assessment of water challenges under uncertainty in water scarcity projections. Nat Sustain 1:486–494
Grippa M, Kergoat L, Boone A, Peugeot C, Demarty J, Cappelaere B, Ducharne A (2017) Modeling surface runoff and water fluxes over contrasted soils in the pastoral sahel: evaluation of the ALMIP2 land surface models over the Gourma Region in Mali. J Hydrometeorol 18:1847–1866
Gunkel A, Lange J (2017) Water scarcity, data scarcity and the Budyko curve—an application in the lower Jordan river basin. J Hydrol: Reg Stud 12:136–149
Hasan E, Tarhule A, Kirstetter P-E, Clark R III, Hong Y (2018) Runoff sensitivity to climate change in the Nile river basin. J Hydrol 561:312–321
Herrera PA, Marazuela MA, Hofmann T (2022) Parameter estimation and uncertainty analysis in hydrological modeling. Wires Water 9:e1569. https://doi.org/10.1002/wat2.1569
Huntington JL, Hegewisch KC, Daudert B, Morton CG, Abatzoglou JT, McEvoy DJ, Erickson T (2017) Climate engine: cloud computing and visualization of climate and remote sensing data for advanced natural resource monitoring and process understanding. Bull Am Meteor Soc 98:2397–2410
Ibrahim SA, Kaduk J, Tansey K, Balzter H, Lawal UM (2021) Detecting phenological changes in plant functional types over West African savannah dominated landscape. Int J Remote Sens 42:567–594. https://doi.org/10.1080/01431161.2020.1811914
Jambou R, Njedanoun M, Panthou G, Descroix L (2022) Malaria transmission in Sahelian African regions, a witness of climate changes. Int J Environ Res Public Health 19:10105
Jellason NP, Conway JS, Baines RN, Ogbaga CC (2021) A review of farming challenges and resilience management in the Sudano-Sahelian drylands of Nigeria in an era of climate change. J Arid Environ 186:104398
Jiang M, Jia L, Menenti M, Zeng Y (2022) Understanding spatial patterns in the drivers of greenness trends in the Sahel-Sudano-Guinean region. Big Earth Data 7:1–20
Kaptué AT, Prihodko L, Hanan NP (2015) On regreening and degradation in Sahelian watersheds. Proc Natl Acad Sci 112:12133–12138
Kaushik PR, Ndehedehe CE, Burrows RM, Noll MR, Kennard MJ (2023) Assessing surface-groundwater interactions for sustaining spring wetlands of the Great Artesian Basin. Aust Ecol Indic 151:110310
Kendall MG (1970). Rank correlation methods (london: Charles griffin, 1948). KendallRank Correlation Methods 1948,
Khan Z, Khan FA, Khan AU, Hussain I, Khan A, Shah LA, Dyczko A (2022) Climate-streamflow relationship and consequences of its instability in large rivers of Pakistan: an elasticity perspective. Water 14:2033
Kingston D, Massei N, Dieppois B, Hannah D, Hartmann A, Lavers D, Vidal J-P (2020) Moving beyond the catchment scale: value and opportunities in large-scale hydrology to understand our changing world. Hydrol Process 34:2292–2298
Lebel T, Ali A (2009) Recent trends in the Central and Western Sahel rainfall regime (1990–2007). J Hydrol 375:52–64
Lehner B, Grill G (2013) Global river hydrography and network routing: baseline data and new approaches to study the world's large river systems. Hydrol Process 27:2171–2186
Li D, Pan M, Cong Z, Zhang L, Wood E (2013) Vegetation control on water and energy balance within the Budyko framework. Water Resour Res 49:969–976
Liu D, Mishra AK, Zhang K (2017) Runoff sensitivity over Asia: Role of climate variables and initial soil conditions. J Geophys Res: Atmos 122:2218–2238
Liu H, Xu C, Allen CD, Hartmann H, Wei X, Yakir D, Yu P (2022) Nature-based framework for sustainable afforestation in global drylands under changing climate. Glob Chang Biol 28:2202–2220
Mann HB (1945) Nonparametric tests against trend. Econometrica: J Econ Soc 13:245–259
McNally A, Arsenault K, Kumar S, Shukla S, Peterson P, Wang S, Verdin JP (2017) A land data assimilation system for sub-Saharan Africa food and water security applications. Sci Data 4:1–19

Mianabadi A, Davary K, Pourreza-Bilondi M, Coenders-Gerrits AMJ (2020) Budyko framework; towards non-steady state conditions. J Hydrol 588:125089
Miller J, Taylor C, Guichard F, Peyrillé P, Vischel T, Fowe T, Traore K (2022) High-impact weather and urban flooding in the West African Sahel–a multidisciplinary case study of the 2009 event in Ouagadougou. Weather Clim Extrem 36:100462
Mirzabaev A, Stringer L, Benjaminsen T, Gonzalez P, Harris R, Jafari M, Zakieldeen S (2022) Cross-chapter paper 3: deserts, semi-arid areas and desertification. Clim Chang 2195–2231
Ndiaye PM, Bodian A, Diop L, Deme A, Dezetter A, Djaman K, Ogilvie A (2020) Trend and sensitivity analysis of reference evapotranspiration in the Senegal river basin using NASA meteorological data. Water 12:1957
Nkiaka E (2022) Water security assessment in ungauged regions using the water balance and water footprint concepts and satellite observations. Hydrol Res 53:336–352. https://doi.org/10.2166/nh.2022.124
Nkiaka E, Okafor GC (2024) Changes in climate, vegetation cover and vegetation composition affect runoff generation in the Gulf of Guinea Basin. Hydrol Process 38:e15124
Nkiaka E, Nawaz NR, Lovett JC (2018) Effect of single and multi-site calibration techniques on hydrological model performance, parameter estimation and predictive uncertainty: a case study in the Logone catchment, Lake Chad basin. Stoch Env Res Risk Assess 32:1665–1682. https://doi.org/10.1007/s00477-017-1466-0
Nkiaka E, Bryant RG, Ntajal J, Biao EI (2022) Evaluating the accuracy of gridded water resources reanalysis and evapotranspiration products for assessing water security in poorly gauged basins. Hydrol Earth Syst Sci 26:5899–5916
Odongo RA, De Moel H, Van Loon AF (2023) Propagation from meteorological to hydrological drought in the Horn of Africa using both standardized and threshold-based indices. Nat Hazards Earth Syst Sci 23:2365–2386
Reaver NGF, Kaplan DA, Klammler H, Jawitz JW (2022) Theoretical and empirical evidence against the Budyko catchment trajectory conjecture. Hydrol Earth Syst Sci 26:1507–1525
Ricciardi L, D'Odorico P, Galli N, Chiarelli DD, Rulli MC (2022) Hydrological implications of large-scale afforestation in tropical biomes for climate change mitigation. Philos Trans R Soc B 377:20210391
Sankarasubramanian A, Vogel RM, Limbrunner JF (2001) Climate elasticity of streamflow in the United States. Water Resour Res 37:1771–1781
Sanogo S, Fink AH, Omotosho JA, Ba A, Redl R, Ermert V (2015) Spatio-temporal characteristics of the recent rainfall recovery in West Africa. Int J Climatol 35:4589–4605
Sen PK (1968) Estimates of the regression coefficient based on Kendall's tau. J Am Stat Assoc 63:1379–1389
Souverijns N, Buchhorn M, Horion S, Fensholt R, Verbeeck H, Verbesselt J, Somers B (2020) Thirty years of land cover and fraction cover changes over the Sudano-Sahel using landsat time series. Remote Sens 12:3817
Tan X, Liu B, Tan X (2020) Global changes in baseflow under the impacts of changing climate and vegetation. Water Resour Res 56:e2020WR027349
Taylor CM, Belušić D, Guichard F, Parker DJ, Vischel T, Bock O, Panthou G (2017) Frequency of extreme Sahelian storms tripled since 1982 in satellite observations. Nature 544:475–478
Tazen F, Diarra A, Kabore RF, Ibrahim B, Bologo/Traoré M, Traoré K, Karambiri H (2019) Trends in flood events and their relationship to extreme rainfall in an urban area of Sahelian West Africa: the case study of Ouagadougou, Burkina Faso. J Flood Risk Manag 12:e12507
Thomas NP, Anyamba A, Tubbs H, Bishnoi B (2022) Evaluation of extreme soil moisture conditions during the 2020 sahel floods and implications for disease outbreaks. Geophys Res Letters 49:e2022GL099872
Tsai Y (2017) The multivariate climatic and anthropogenic elasticity of streamflow in the Eastern United States. J Hydrol: Reg Stud 9:199–215
Vizy EK, Cook KH (2022) Distribution of extreme rainfall events and their environmental controls in the West African Sahel and Soudan. Clim Dyn 59:1–30
Wamucii CN, van Oel PR, Ligtenberg A, Gathenya JM, Teuling AJ (2021) Land use and climate change effects on water yield from East African forested water towers. Hydrol Earth Syst Sci 25:5641–5665
Wendling V, Peugeot C, Mayor AG, Hiernaux P, Mougin E, Grippa M, Lebel T (2019) Drought-induced regime shift and resilience of a Sahelian ecohydrosystem. Environ Res Lett 14:105005
Wu H, Chen B, Ye X, Guo H, Meng X, Zhang B (2021) An improved calibration and uncertainty analysis approach using a multicriteria sequential algorithm for hydrological modeling. Sci Rep 11:16954. https://doi.org/10.1038/s41598-021-96250-6
Wu G, Lu X, Zhao W, Cao R, Xie W, Wang L, Li S (2023) The increasing contribution of greening to the terrestrial evapotranspiration in China. Ecol Model 477:110273
Yonaba R, Biaou AC, Koïta M, Tazen F, Mounirou LA, Zouré CO, Yacouba H (2021) A dynamic land use/land cover input helps in picturing the Sahelian paradox: assessing variability and attribution of changes in surface runoff in a Sahelian watershed. Sci Total Environ 757:143792
Yonaba R, Mounirou LA, Tazen F, Koïta M, Biaou AC, Zouré CO, Yacouba H (2023) Future climate or land use? Attribution of changes in surface runoff in a typical Sahelian landscape. Comptes Rendus Géosci 355:1–28
Zhang Y, Zheng H, Zhang X, Leung LR, Liu C, Zheng C, Blöschl G (2023) Future global streamflow declines are probably more severe than previously estimated. Nature Water. https://doi.org/10.1038/s44221-023-00030-7doi:10.1038/s44221-023-00030-7
Zheng H, Zhang L, Zhu R, Liu C, Sato Y, Fukushima Y (2009) Responses of streamflow to climate and land surface change in the headwaters of the Yellow River Basin. Water Res Res. https://doi.org/10.1029/2007WR006665
Zhou S, Williams AP, Lintner BR, Berg AM, Zhang Y, Keenan TF, Gentine P (2021) Soil moisture–atmosphere feedbacks mitigate declining water availability in drylands. Nat Clim Chang 11:38–44
Zoungrana BJB, Conrad C, Thiel M, Amekudzi LK, Da ED (2018) MODIS NDVI trends and fractional land cover change for improved assessments of vegetation degradation in Burkina Faso, West Africa. J Arid Environ 153:66–75